

Emergence and Violation of Geometrical Scaling in pp Collisions[§]

Michal Praszalowicz*

M. Smoluchowski Institute of Physics, Jagellonian University, Reymonta 4, 30-059 Krakow, Poland

Abstract: We argue that geometrical scaling (GS) proposed originally in the context of Deep Inelastic Scattering (DIS) at HERA works also in pp collisions at the LHC energies and in NA61/SHINE experiment. We show that in DIS GS is working up to relatively large Bjorken $x \sim 0.1$. As a consequence negative pion multiplicity p_T distributions at NA61/SHINE energies exhibit GS in mid rapidity region. For $y \neq 0$ clear sign of scaling violations can be seen when one of the colliding partons has Bjorken $x \geq 0.1$. Finally, we argue that in the case of identified particles GS scaling is still present but the scaling variable is a function of transverse mass rather than p_T .

PACS number(s): 13.85.Ni, 12.38.Lg.

Keywords: Gluon saturation, low x physics, geometrical scaling.

1. INTRODUCTION

This talk based on refs. [1-6] (where also an extensive list of references can be found) follows closely an earlier report of ref. [7]. We shall discuss the scaling law, called geometrical scaling (GS), which has been introduced in the context of DIS [8]. It has been also shown that GS is exhibited by the p_T spectra at the LHC [1, 3] and that an onset of GS can be seen in heavy ion collisions at RHIC energies [3]. At low Bjorken $x < x_{\max}$ gluonic cloud in the proton is characterized by an intermediate energy scale $Q_s(x)$, called saturation scale [9, 10]. $Q_s(x)$ is defined as the border line between dense and dilute gluonic systems (for review see *e.g.* refs. [11, 12]). In the present paper we study the consequences of the very existence of $Q_s(x)$; the details of saturation phenomenon are here not of primary importance.

Here we shall focus of four different pieces of data which exhibit both emergence and violation of geometrical scaling. In Sect. 2 we briefly describe the method used to assess the existence of GS. Secondly, in Sect. 3 we describe our recent analysis [4] of combined HERA data [13] where it has been shown that GS in DIS works surprisingly well up to relatively large $x_{\max} \sim 0.1$ (see also [14]). Next, in Sect. 4, on the example of the CMS p_T spectra in central rapidity [15], we show that GS is also present in hadronic collisions. For particles produced at non-zero rapidities, one (larger) Bjorken $x = x_1$ may be outside of the domain of GS, *i.e.*

$x_1 > x_{\max}$, and violation of GS should appear. In Sect. 5 we present analysis of the pp data from NA61/SHINE experiment at CERN [16] and show that GS is indeed violated once rapidity is increased. Finally in Sect. 6 we analyze identified particles spectra where the particle mass provides another energy scale which may lead to the violation of GS, or at least to some sort of its modification [6]. We conclude in Sect. 7.

2. ANALYZING DATA WITH METHOD OF RATIOS

Geometrical scaling hypothesis means that some observable σ depending in principle on two independent kinematical variables, like x and Q^2 , depends in fact only on a given combination of them, denoted in the following as τ :

$$\sigma(x, Q^2) = F(\tau) / Q_0^2. \quad (1)$$

Here function F in Eq. (1) is a dimensionless universal function of scaling variable τ :

$$\tau = Q^2 / Q_s^2(x). \quad (2)$$

and

$$Q_s^2(x) = Q_0^2 (x / x_0)^{-\lambda} \quad (3)$$

is the saturation scale. Here Q_0 and x_0 are free parameters which, however, are not of importance in the present analysis, and exponent λ is a dynamical quantity of the order of $\lambda \sim 0.3$. Throughout this paper we shall test the hypothesis whether different pieces of data can be described by formula (1) with *constant* λ , and what is the kinematical range where GS is working satisfactorily.

As a consequence of Eq. (1) observables $\sigma(x_i, Q^2)$ for different x_i 's should fall on a universal curve, if evaluated in terms of scaling variable τ . This means that ratios

*Address correspondence to this author at the Institute of Physics, Jagellonian University, Reymonta 4, 30-059 Krakow, Poland; Tel: +48 12 663 56 77; Fax: +48 12 633 40 79; E-mail: michal@if.uj.edu.pl

[§]Presented at the Low x Workshop, May 30 - June 4 2013, Rehovot and Eilat, Israel.

$$R_{x_i \rightarrow x_{\text{ref}}}(\lambda; \tau_k) = \frac{\sigma(x_i, \tau(x_i, Q_k^2; \lambda))}{\sigma(x_{\text{ref}}, \tau(x_{\text{ref}}, Q_{k,\text{ref}}^2; \lambda))} \quad (4)$$

should be equal to unity independently of τ . Here for some x_{ref} we pick up all $x_i < x_{\text{ref}}$ which have at least two overlapping points in Q^2 .

For $\lambda \neq 0$ points of the same Q^2 but different x 's correspond in general to different τ 's. Therefore one has to interpolate $\sigma(x_{\text{ref}}, \tau(x_{\text{ref}}, Q^2; \lambda))$ to $Q_{k,\text{ref}}^2$ such that $\tau(x_{\text{ref}}, Q_{k,\text{ref}}^2; \lambda) = \tau_k$. This procedure is described in detail in ref. [4].

By adjusting λ one can make $R_{x_i \rightarrow x_{\text{ref}}}(\lambda; \tau_k) \rightarrow 1$ for all τ_k in a given interval. In order to find an optimal value λ_{min} which minimizes deviations of ratios (4) from unity we form the chi-square measure

$$\chi_{x_i \rightarrow x_{\text{ref}}}^2(\lambda) = \frac{1}{N_{x_i \rightarrow x_{\text{ref}}}} \sum_{k \in x_i} \frac{(R_{x_i \rightarrow x_{\text{ref}}}(\lambda; \tau_k) - 1)^2}{\Delta R_{x_i \rightarrow x_{\text{ref}}}(\lambda; \tau_k)^2} \quad (5)$$

where the sum over k extends over all points of given x_i that have overlap with x_{ref} , and $N_{x_i \rightarrow x_{\text{ref}}}$ is a number of such points.

3. GEOMETRICAL SCALING IN DIS AT HERA

In the case of DIS the relevant scaling observable is $\gamma^* p$ cross section and variable x is simply Bjorken x . In Fig. (1) we present 3-d plot of $\lambda_{\text{min}}(x, x_{\text{ref}})$ which has been found by minimizing (5).

Qualitatively, GS is given by the independence of λ_{min} on Bjorken x and by the requirement that the respective value of $\chi_{x, x_{\text{ref}}}^2(\lambda_{\text{min}})$ is small (for more detailed discussion see ref. [4]). One can see from Fig. (1) that the stability corner of λ_{min} extends up to $x_{\text{ref}} \sim 0.1$, which is well above the original expectations. In ref. [4] we have shown that:

$$\lambda = 0.32 - 0.34 \text{ for } x \leq 0.08. \quad (6)$$

4. GEOMETRICAL SCALING OF CENTRAL RAPIDITY p_T SPECTRA AT THE LHC

In hadronic collisions at c.m. energy $W = \sqrt{s}$ particles are produced in the scattering process of two patrons (mainly gluons) carrying Bjorken x 's

$$x_{1,2} = e^{\pm y} p_T / W. \quad (7)$$

For central rapidities $x = x_1 \sim x_2$. In this case charged particles multiplicity spectra exhibit GS [1]

$$\left. \frac{dN}{dy d^2 p_T} \right|_{y=0} = \frac{1}{Q_0^2} F(\tau) \quad (8)$$

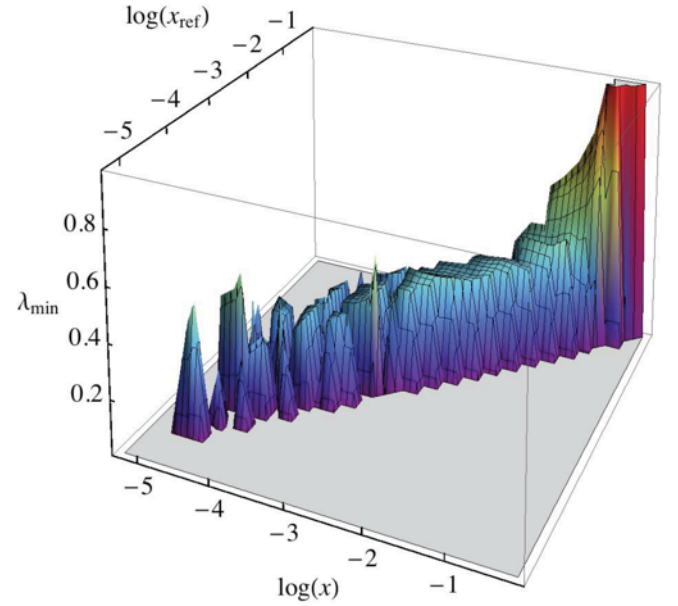


Fig. (1). Three dimensional plot of $\lambda_{\text{min}}(x, x_{\text{ref}})$ obtained by minimization of Eq. (5).

where F is a universal dimensionless function of the scaling variable (2). Therefore the method of ratios can be applied to the multiplicity distributions at different energies (W_i taking over the role of x_i in Eq. (4))¹. For W_{ref} we take the highest LHC energy of 7 TeV. Hence one can form two ratios R_{W_{ref}, W_i} with $W_1 = 2.36$ and $W_2 = 0.9$ TeV. These ratios are plotted in Fig. (2) for the CMS single non-diffractive spectra for $\lambda = 0$ and for $\lambda = 0.27$, which minimizes (5) in this case. We see that original ratios plotted in terms of p_T range from 1.5 to 7, whereas plotted in terms of $\sqrt{\tau}$ they are well concentrated around unity. The optimal exponent λ is, however, smaller than in the case of DIS. Why this so, remains to be understood.

5. VIOLATION OF GEOMETRICAL SCALING IN FORWARD RAPIDITY REGION

For $y > 0$ two Bjorken x 's can be quite different: $x_1 > x_2$. Therefore by increasing y one can eventually reach $x_1 > x_{\text{max}}$ and GS violation should be seen. For that purpose we shall use pp data from NA61/SHINE experiment at CERN [16] at different rapidities $y = 0.1 - 3.5$ and at five scattering energies $W_{1, \dots, 5} = 17.28, 12.36, 8.77, 7.75$, and 6.28 GeV.

In Fig. (3) we plot ratios $R_{li} = R_{W_1, W_i}$ (4) for π^- spectra in central rapidity for $\lambda = 0$ and 0.27. For $y = 0.1$ the GS region extends down to the smallest energy because x_{max} is as large as 0.08. However, the quality of GS is the worst for the lowest energy W_5 . By increasing y some points fall

¹For pp collisions we define ratios R_{W_{ref}, W_i} as an inverse of (4).

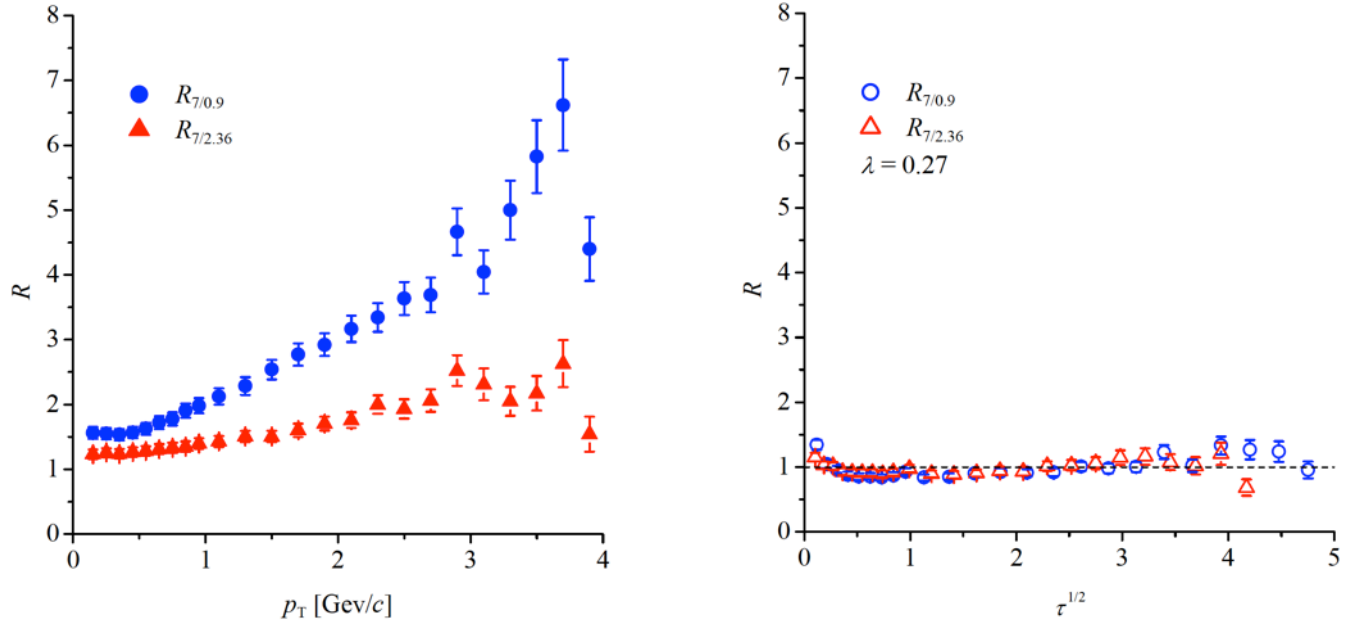


Fig. (2). Ratios of CMS p_T spectra [15] at 7 TeV to 0.9 (blue circles) and 2.36 TeV (red triangles) plotted as functions of p_T (left) and scaling variable $\sqrt{\tau}$ (right) for $\lambda = 0.27$.

outside the GS window because $x_1 \geq x_{\max}$, and finally for $y \geq 1.7$ no GS is present in NA61/SHINE data. This is illustrated nicely in Fig. (4).

6. GEOMETRICAL SCALING FOR IDENTIFIED PARTICLES

In ref. [6] we have proposed that in the case of identified particles another scaling variable should be used in which p_T is replaced by $\tilde{m}_T = m_T - m = \sqrt{m_T^2 + p_T^2} - m$ (\tilde{m}_T -scaling), *i.e.*

$$\tau_{\tilde{m}_T} = \frac{\tilde{m}_T^2}{Q_0^2} \left(\frac{\tilde{m}_T}{x_0 W} \right)^\lambda. \quad (9)$$

This choice is purely phenomenological for the following reasons. Firstly, the gluon cloud is in principle not sensitive to the mass of the particle it finally is fragmenting to, so in principle one should take p_T as an argument of the saturation scale. In this case the proper scaling variable would be

$$\tau_{\tilde{m}_T p_T} = \frac{\tilde{m}_T^2}{Q_0^2} \left(\frac{p_T}{x_0 W} \right)^\lambda. \quad (10)$$

However this choice ($\tilde{m}_T p_T$ -scaling) does not really differ numerically from the one given by Eq. (9).

To this end let us see how scaling properties of GS are affected by going from scaling variable $\tau_{p_T} = \tau$ (2) to $\tau_{\tilde{m}_T}$ (9) and what would be the difference in scaling properties if we had

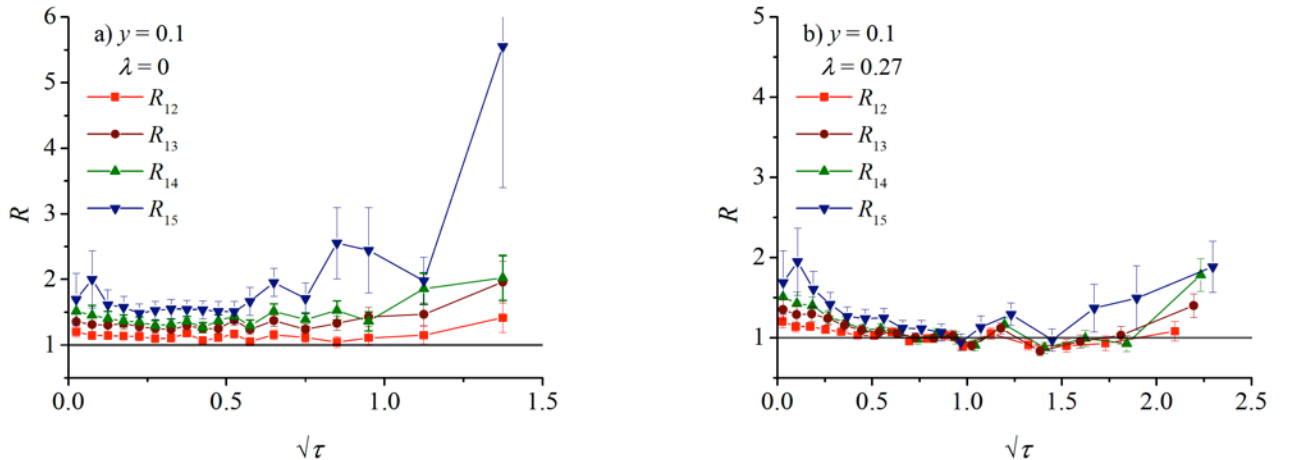


Fig. (3). Ratios R_{1k} as functions of $\sqrt{\tau}$ for the lowest rapidity $y = 0.1$: a) for $\lambda = 0$ when $\sqrt{\tau} = p_T$ and b) for $\lambda = 0.27$ which corresponds to GS.

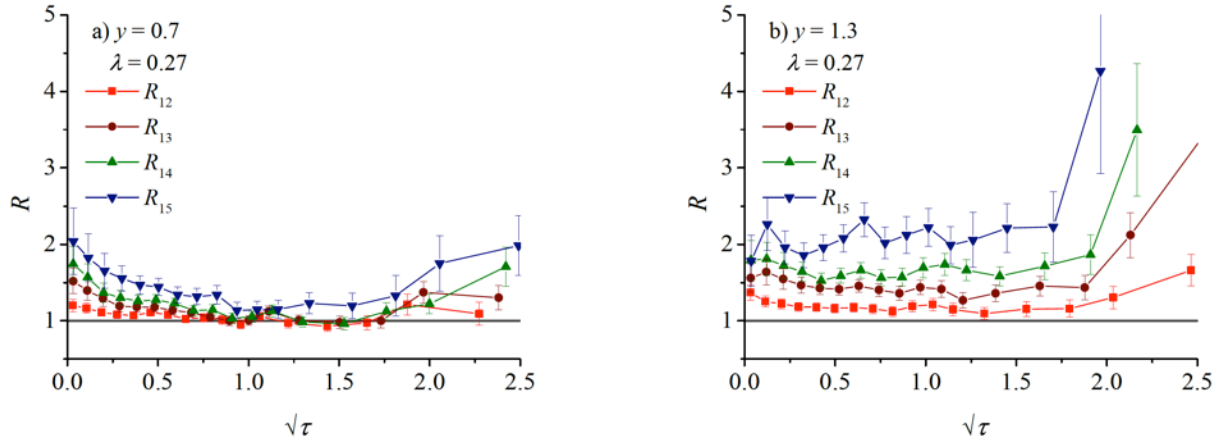


Fig. (4). Ratios R_{ik} as functions of $\sqrt{\tau}$ for $\lambda=0.27$ and for different rapidities a) $y=0.7$ and b) $y=1.3$. With increase of rapidity, gradual closure of the GS window can be seen.

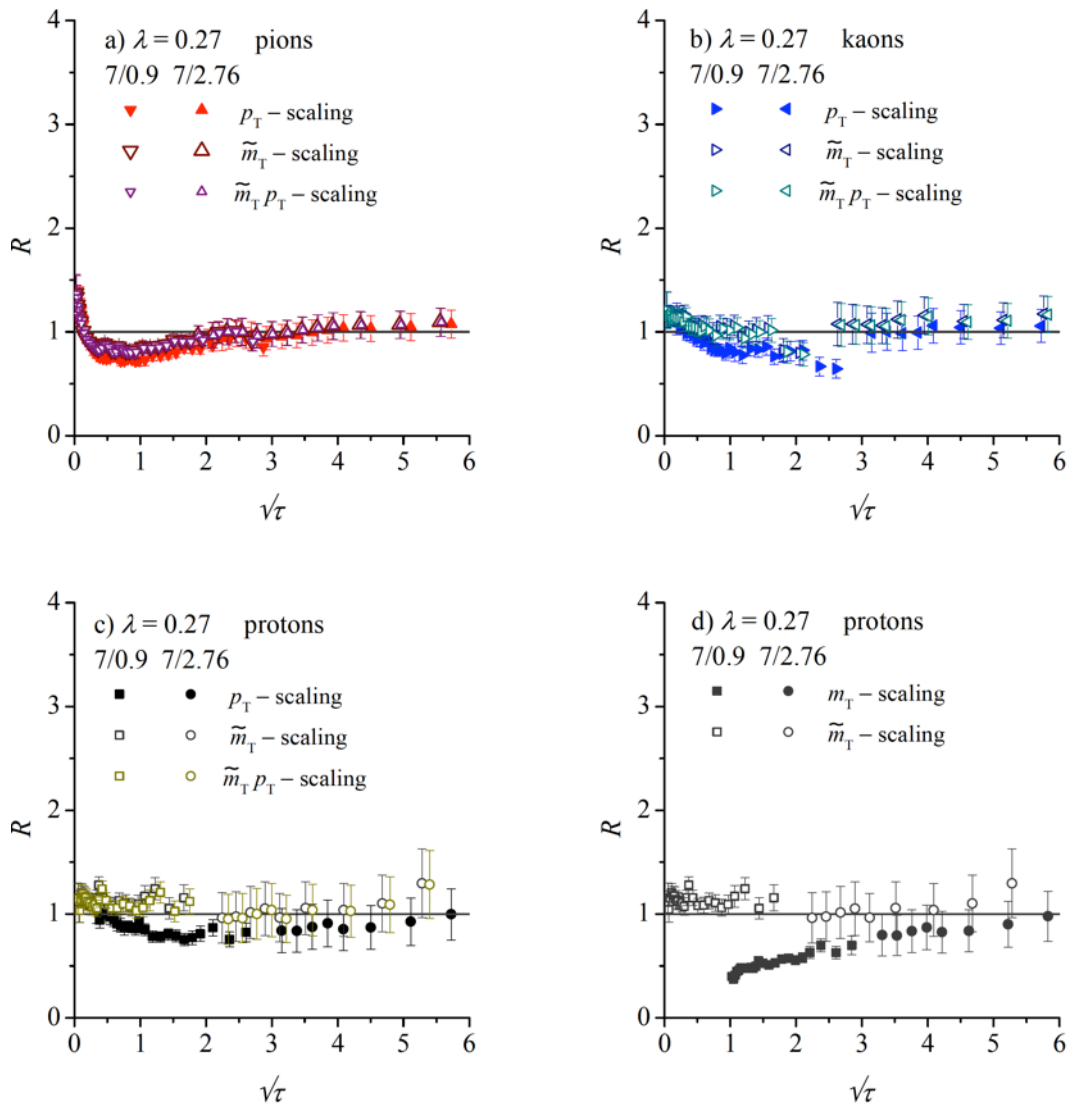


Fig. (5). Panels a) - c): comparison of geometrical scaling in three different variables: τ_{p_T} , $\tau_{\tilde{m}_T}$ and $\tau_{\tilde{m}_T p_T}$ for $\lambda=0.27$. Full symbols correspond to ratios R_{W_1/W_2} plotted in terms of the scaling variable τ_{p_T} , open symbols to $\tau_{\tilde{m}_T}$ and $\tau_{\tilde{m}_T p_T}$, note negligible differences between the latter two forms of scaling variable. Panel a) corresponds to pions, b) to kaons and c) to protons. In panel d) we show comparison of geometrical scaling for protons in scaling variables $\tau_{\tilde{m}_T}$ and τ_{m_T} , no GS can be achieved in the latter case.

chosen p_T as an argument in the saturation scale leading to scaling variable $\tau_{\tilde{m}_T p_T}$ (10). This is illustrated in Fig. (5) where we show analysis [6] of recent ALICE data on identified particles [17]. In Fig. (5a-c) full symbols refer to the p_T – scaling (2) and open symbols to \tilde{m}_T – scaling or $\tilde{m}_T p_T$ – scaling. One can see very small difference between open symbols indicating that scaling variables $\tau_{\tilde{m}_T}$ (9) and $\tau_{\tilde{m}_T p_T}$ (10) exhibit GS of the same quality. On the contrary p_T – scaling in variable τ_{p_T} (2) is visibly worse.

Finally in Fig. (5d), on the example of protons, we compare \tilde{m}_T – scaling (open symbols) and m_T – scaling (full symbols) in variable

$$\tau_m = \frac{m_T^2}{Q_0^2} \left(\frac{m_T}{x_0 W} \right)^\lambda. \quad (11)$$

for $\lambda = 0.27$. One can see that no GS has been achieved in the latter case. Qualitatively the same behavior can be observed for other values of λ .

7. CONCLUSIONS

In ref. [4] we have shown that GS in DIS works well up to rather large Bjorken x 's with exponent $\lambda = 0.32 - 0.34$. In pp collisions at the LHC energies in central rapidity GS is seen in the charged particle multiplicity spectra, however, $\lambda = 0.27$ in this case [1]. By changing rapidity one can force one of the Bjorken x 's of colliding partners to exceed x_{\max} and GS violation is expected. Such behavior is indeed observed in the NA61/SHINE pp data [5]. Finally we have shown that for identified particles scaling variable τ of Eq. (2) should be replaced by $\tau_{\tilde{m}_T}$ defined in Eq. (9) and the scaling exponent $\lambda \approx 0.3$ [6].

CONFLICT OF INTEREST

The authors confirm that this article content has no conflicts of interest.

ACKNOWLEDGEMENTS

Many thanks are due to the organizers of this successful series of conferences. This work was supported by the Polish NCN grant 2011/01/B/ST2/00492.

REFERENCES

- [1] (a). McLerran L, Praszalowicz M. Saturation and scaling of multiplicity, mean p_T and p_T distributions from 200 GeV < \sqrt{s} < 7

- TeV. Acta Phys Pol B 2010; 41: 1917-26. (b). Saturation and dealing of multiplicity, mean p_T and p_T distributions from 200 GeV < \sqrt{s} < 7 TeV – Addendum. Acta Phys Pol B 2011; 42: 99-103.
- [2] Praszalowicz M. Improved geometrical scaling at the LHC. Phys Rev Lett 2011; 106: 142002.
- [3] (a). Praszalowicz M. Geometrical scaling in hadronic collisions. Acta Phys Pol B 2011; 42: 1557-66. (b). Geometrical Scaling in in High Energy Hadronic Collisions. [arXiv:1205.4538 [hep-ph]].
- [4] (a). Praszalowicz M, Stebel T. Quantitative study of geometrical scaling in deep inelastic scattering at HERA. J High Energy Phys 2013; 1303: 090. (b). Quantitative study of different forms of geometrical scaling in deep inelastic scattering at HERA. J High Energy Phys 2013; 1304: 169.
- [5] Praszalowicz M. Violation of geometrical scaling in pp collisions at NA61/SHINE. Phys Rev D 2013; 87: 071502(R).
- [6] Praszalowicz M. Geometrical scaling for identified particles. Phys Lett B 2013; 727: 461-7.
- [7] Praszalowicz M. Geometrical scaling in high energy collisions and its breaking. Acta Phys Pol B Proceeding Suppl 2013; 6: 809-16.
- [8] Stasto AM, Golec-Biernat KJ, Kwiecinski J. Geometric scaling for the total gamma p cross section in the low x region. Phys Rev Lett 2001; 86: 596-9.
- [9] (a). Gribov LV, Levin EM, Ryskin MG. Semihard processes in QCD. Phys Rept 1983; 100: 1-150. (b). Mueller AH, Qiu JW. Gluon recombination and shadowing at Small Values of x. Nucl Phys 1986; 268: 427-52. (c). Mueller AH. Parton saturation at small x and in large nuclei. Nucl Phys 1999; B558: 285-303.
- [10] (a). Golec-Biernat KJ, Wüsthoff M. Saturation effects in deep inelastic scattering at low Q**2 and its implications on diffraction. Phys Rev D 1998; 59: 014017. (b). Saturation in diffractive deep inelastic scattering. Phys Rev D 1999; 60: 114023.
- [11] Mueller AH. Parton Saturation: An Overview. [arXiv:hep-ph/0111244].
- [12] McLerran L. Matter at very high energy density: 3 Lectures in Zakopane. Acta Phys Pol B 2010; 41: 2799-26.
- [13] (a). Adloff C, Andreev V, Andrieu B, et al. [H1 Collaboration]. Deep-inelastic inclusive ep scattering at low x and a determination of alpha_s. Eur Phys J C 2001; 21: 33-61. (b). Chekanov S, Derrick M, Krakauer D, et al. [ZEUS Collaboration]. Measurement of the neutral current cross section and F_2 structure function for deep inelastic e+ p scattering at HERA. Eur Phys J C 2001; 21: 443-71.
- [14] Caola F, Forte S, Rojo J. HERA data and DGLAP evolution: Theory and phenomenology. Nucl Phys A 2011; 854: 32-44.
- [15] (a). Khachatryan V, Sirunyan AM, Tumasyan A, et al. [CMS Collaboration]. Transverse momentum and pseudorapidity distributions of charged hadrons in pp collisions at $\sqrt{s} = 0.9$ and 2.36 TeV. J High Energy Phys 2010; 1002: 041. (b). Transverse-momentum and pseudorapidity distributions of charged hadrons in pp collisions at $\sqrt{s} = 7$ TeV. Phys Rev Lett 2010; 105: 022002. (c). Charged particle multiplicities in pp interactions at $\sqrt{s} = 0.9, 2.36,$ and 7 TeV. J High Energy Phys 2011; 1101: 079.
- [16] (a). Abgrall N, Aduszkiewicz A, Antićić T, et al. [NA61/SHINE Collaboration]. Report from the NA61/SHINE experiment at the CERN SPS CERN-SPSC-2012-029, SPSC-SR-107. (b). Aduszkiewicz A. Ph.D. Thesis, University of Warsaw 2013. (c). Pulawski S. Talk at 9th Polish workshop on Relativistic Heavy-Ion Collisions, Kraków, November 2012 and private communication.
- [17] (a). Aamodt K, Abel N, Abeyssekara U, et al. [ALICE Collaboration]. Production of pions, kaons and protons in pp collisions at $\sqrt{s} = 900$ GeV with ALICE at the LHC. Eur Phys J C 2011; 71: 1655. (b). Velasquez AO. [ALICE Collaboration]. Production of pions, kaons and protons at high p_T in $\sqrt{s_{NN}} = 2.76$ TeV Pb-Pb collisions. Nucl Phys A 2013; 904-905: 763c-766c (ALICE preliminary).

Received: November 25, 2013

Revised: January 29, 2014

Accepted: January 30, 2014

© Michal Praszalowicz; Licensee Bentham Open.

This is an open access article licensed under the terms of the Creative Commons Attribution Non-Commercial License (<http://creativecommons.org/licenses/by-nc/3.0/>) which permits unrestricted, non-commercial use, distribution and reproduction in any medium, provided the work is properly cited.